Veneer Stability Evaluation of a Geosynthetic Cover System for Mine Waste Rock

Kyle Howse & I.R. Fleming
Department of Civil, Geological, and Environmental Engineering – University of Saskatchewan, Saskatoon, Saskatchewan, Canada

GeoCalgary 2022 October 2-5 Reflection on Resources

ABSTRACT
Geomembranes have the potential to be effective barriers in cover systems for mine rock to reduce the influx of atmospheric water and oxygen. However, concerns related to constructability and long-term performance have been a factor in preventing the adoption of this method. The veneer stability of a typical geosynthetic cover system is evaluated for a site containing mine rock composed of shale and limestone. Direct and interface shear tests were completed to measure the angle of internal shearing resistance for soil used in the cover and the angle of interface shearing resistance between each of the potential geosynthetic-geosynthetic and soil-geosynthetic interfaces. The results from this work can assist in the selection of geosynthetic materials and the design slope for a geosynthetic cover system.

RÉSUMÉ
Les géomembranes ont le potentiel d'être des barrières efficaces dans les systèmes de couverture pour les roches de mine afin de réduire l'afflux d'eau et d'oxygène atmosphériques. Cependant, les préoccupations liées à la constructibilité et aux performances à long terme ont été un facteur empêchant l'adoption de cette méthode. La stabilité du placage d'un système de couverture géosynthétique typique est évaluée pour un site contenant de la roche de mine composée de schiste et de calcaire. Des essais de cisaillement direct et d'interface ont été effectués pour mesurer l'angle de résistance au cisaillement interne du sol utilisé dans la couverture et l'angle de résistance au cisaillement de l'interface entre chacune des interfaces potentielles géosynthétique-géosynthétique et sol-géosynthétique. Les résultats de ce travail peuvent aider à la sélection des matériaux géosynthétiques et à la pente de conception d'un système de couverture géosynthétique.

1 INTRODUCTION

Mining projects around the world are presented with the challenge of managing large volumes of waste rock produced during mining operations. Environmental risks associated with this material typically result from acid rock drainage (ARD) caused by oxidizing sulphide minerals, or neutral drainage (ND) containing high concentrations of salinity and/or dissolved metals (MEND, 2012). Storing this rock at the surface has the potential to cause the transport of contaminants into the receiving environment.

A common method of minimizing the environmental impact of ARD or ND is to construct a cover on a waste rock pile. A barrier-type cover system uses a low hydraulic conductivity layer to reduce the intrusion of water and oxygen into the waste rock pile to slow down the rates of contaminant generation and contaminant transport (MEND, 2012). The barrier layer is often made from a compacted clay liner (CCL), a compacted sand-bentonite mixture, or a permanently frozen layer (MEND, 2012). The use of a geomembrane in a barrier-type cover system has been explored in recent years (e.g., Power et al., 2017; Ramasamy et al., 2018). However, additional research regarding concerns relating to constructability and long-term performance will be useful in providing mine operators confidence in selecting geomembrane-based cover systems for future projects.

This paper discusses the evaluation of the veneer stability for a typical geosynthetic cover system design for mine waste rock. A series of direct and interface shear tests were completed to measure the angle of internal shearing resistance (ϕ) for soil used in the cover and the angle of interface shearing resistance (δ) between each of the potential geosynthetic-geosynthetic and soil-geosynthetic interfaces. The results of this work can assist in the selection of geosynthetic materials and the design slope for the waste rock pile and cover system.

2 BACKGROUND

2.1 Proposed Cover Design

A typical geosynthetic-based cover system design is presented in Figure 1. A bedding layer of screened waste rock (SWR) is placed over the rough surface of the waste rock pile to provide a reasonable working surface and to mitigate damage caused to the geomembrane from below. A geomembrane is then be placed on the bedding layer. A planar drainage geocomposite (PDG) will be placed on the geomembrane as a protection layer and to intercept some infiltration that could enter the pile through defects in the geomembrane. The PDG will be overlain by a second lift of SWR to act as ballast and protect the underlying geosynthetics.

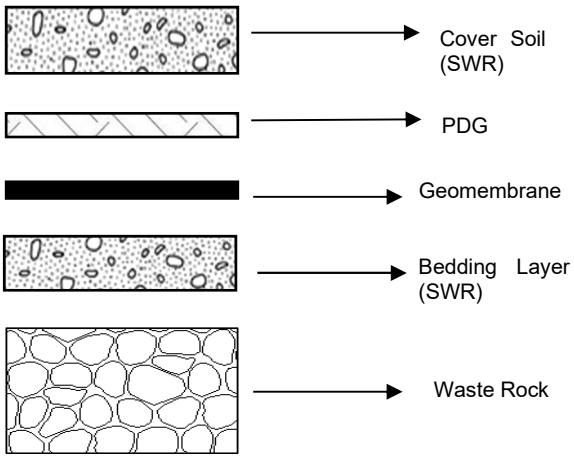

Figure 1. Elements of a typical waste rock pile cover system

2.2 Mohr-Coulomb Failure Envelopes

Geosynthetic-geosynthetic interfaces tested in this research exhibit behaviour modeled by the Mohr-Coulomb model (Eq.1) where τ is the shear stress, σ is the normal stress, δ is the interface friction angle, and a is adhesion.

$$\tau = \sigma \tan \delta + a \quad [1]$$

Direct shear testing of the studied soil was modeled by a second variation of the Mohr-Coulomb equation (Eq. 2) where τ is the shear stress, σ is the normal stress, ϕ is the angle of internal shearing resistance, and c is cohesion.

$$\tau = \sigma \tan \phi + c \quad [2]$$

2.3 Geosynthetic Interface Testing

Geomembrane-soil, geomembrane-geotextile, and geotextile-soil interfaces are commonly present in other engineering applications. Recent studies by Bacas et al. (2015) and Cen et al. (2018) measured the friction angle of several interfaces including textured geomembrane and soil, textured geomembrane and geotextile, and textured geomembrane and geocomposite. These studies found that the geomembrane-geotextile and geomembrane-geocomposite interfaces had lower friction angles than geomembrane-soil interfaces. Increasing asperity height of textured geomembranes has been found to cause increased interlocking on the geomembrane surface resulting in increased shear strength (Bacas et al., 2015; Fowmes et al., 2017; Adeleke et al., 2021; Abdelaal and Solanki, 2022).

3 MATERIALS

3.1 Screened Waste Rock

Mine waste rock was provided from a mine site in Canada. The bedding layer and cover soil is mainly composed of friable shale with some limestone, with particle size less than 25 mm. The particle size distribution for this material is presented in Figure 2.

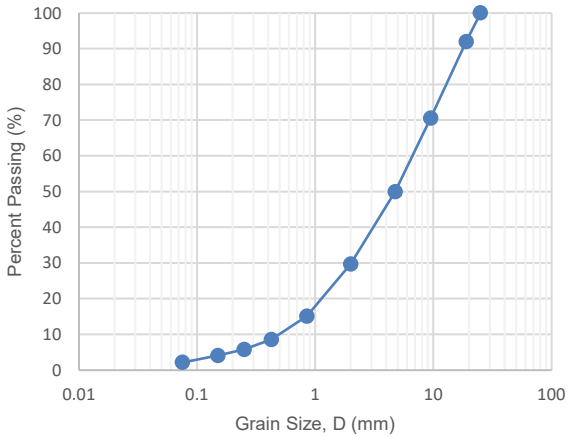

Figure 2. Particle size distribution curve of the mine waste rock

3.2 Geomembranes

Geomembrane materials included high density polyethylene (HDPE) and linear low density polyethylene (LLDPE). All geomembranes were 60 mils thick and textured on both sides. Table 1 presents the different geomembranes evaluated for potential use in the cover system. All geomembranes were manufactured by the same company, but they were provided from different factories in Canada, the US and overseas. Geomembranes with different asperity heights were selected for testing. Figure 3 shows the textured surface of geomembranes with different asperity heights.

Table 1. Characteristics of geomembranes considered for use in the cover system

Material	Thickness (mil)	Asperity Height (mm)
HDPE	60	16
HDPE	60	20
HDPE	60	28
LLDPE	60	16
LLDPE	60	20
LLDPE	60	28

a)

b)

c)

Figure 3. Photos of different textured geomembranes a) 16 mils asperity HDPE, b) 20 mils asperity HDPE, c) 28 mils asperity HDPE

3.3 PDG

The PDG selected for this project is a combination of a nonwoven polyester filter needle-punched to a nonwoven polypropylene drainage blanket. Perforated polypropylene tubes run along pockets between the filter and drainage blanket. Figure 4 shows the components of the PDG.

Figure 4. Photo of the PDG with filter, drainage blanket, and perforated pipes

4 DIRECT SHEAR TESTING

ASTM-D5321 was used to evaluate each of the potential soil-geosynthetic and geosynthetic-geosynthetic interfaces within the proposed cover system using different geomembrane materials and asperity heights. A DGSI LG-8000 large-format direct shear apparatus was used to measure the shear strength of each interface.

The main components of the apparatus include a lower movable box (305 mm x 406 mm x 102 mm) and a fixed upper box (305 mm x 305 mm x 102 mm). The placement of the materials in the apparatus for each test was selected to replicate field conditions. SWR was placed in the bottom box, followed by geosynthetics clamped in place on the surface of the SWR and/or secured within the top box. SWR was again placed in the top box overlying the geosynthetics and covered with a loading platen. Figure 5 shows an example test configuration. An air-operated loading device was used to apply normal loads to the materials.

Tests were performed at normal stresses of 20 kPa, 30 kPa, and 40 kPa for each interface. Linear variable differential transformers (LVDTs) were used to measure the displacement of the bottom box and the loading platen. After applying the normal load, the materials were left to equilibrate for 10 minutes before shearing. All tests were performed under dry conditions.

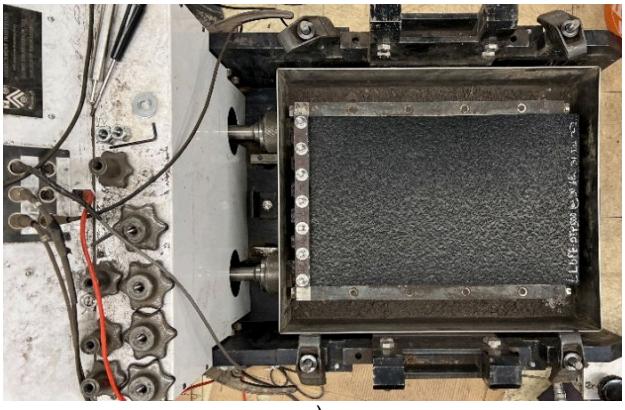

a)

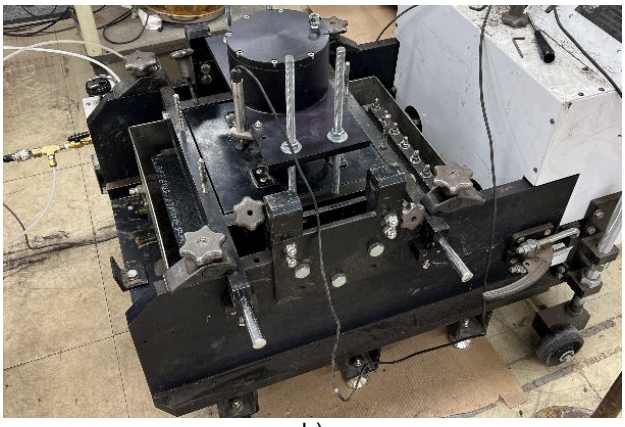

b)

Figure 5. Test configuration for the geomembrane-SWR interface, a) geomembrane clamped in place overlying the SWR layer, b) fully assembled interface shear test

4.1 Selection of displacement rates

For the geomembrane-SWR and SWR-PDG interface the ASTM-D5321 recommended displacement rate of 1 mm/min was used. A displacement rate of 5 mm/min was selected for the geomembrane-PDG interface according to Bacas et al. (2015) and previous studies showing that the displacement rate for geomembrane and geotextile interfaces do not significantly affect the peak shear strength measured in direct shear tests (Stark et al., 1996; Triplett and Fox, 2001).

5 RESULTS

Shear stress vs. horizontal displacement was recorded during direct shear tests at normal loads of 20 kPa, 30 kPa, and 40 kPa for each interface. Figure 6 shows a typical set of shear stress vs. horizontal displacement plots for the 28 mils asperity HDPE geomembrane and SWR interface.

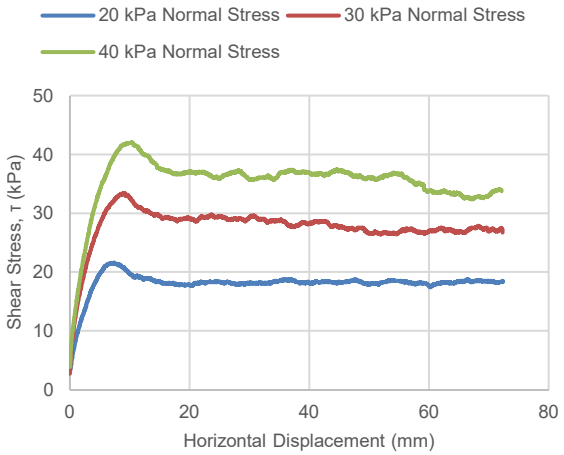

Figure 6. Sample shear stress vs. horizontal displacement plots for the 28 mils asperity HDPE geomembrane and SWR interface

5.1 SWR Internal Friction Angle

Results of the direct shear tests for the SWR are presented in Figure 7. Plotting a best fit line through the origin measures an internal friction angle of 51°.

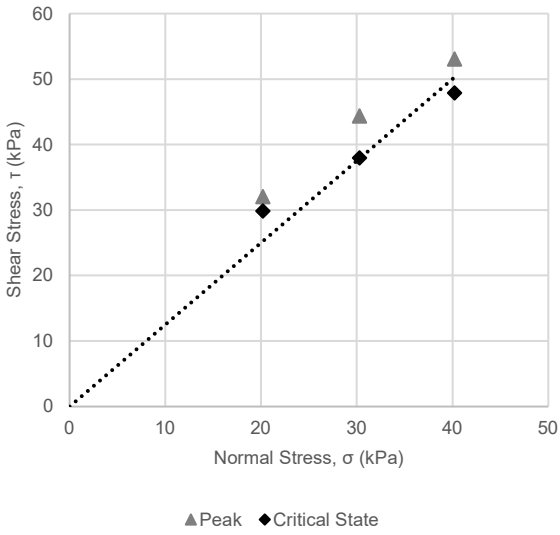

Figure 7. Shear stress vs. normal stress plot for the SWR

5.2 SWR and Geosynthetic Interfaces

Interface shear test results between the SWR and geomembranes showed the interface friction angle ranged from 38° for the 20 mils asperity HDPE geomembrane to 42° for the 28 mils asperity HDPE geomembrane. Dilation behaviour at lower normal stress was observed with inferred dilation angles ranging from 6° to 11°. The PDG and SWR interface tests resulted in an interface friction angle of 43°.

Figure 8 shows a typical plot of peak shear stress vs normal stress for a SWR and geosynthetic interface with the dilation angle measured as the angle between the critical state trend line and peak shear stress points. A summary of the results for the SWR and geosynthetic interfaces is shown in Table 2.

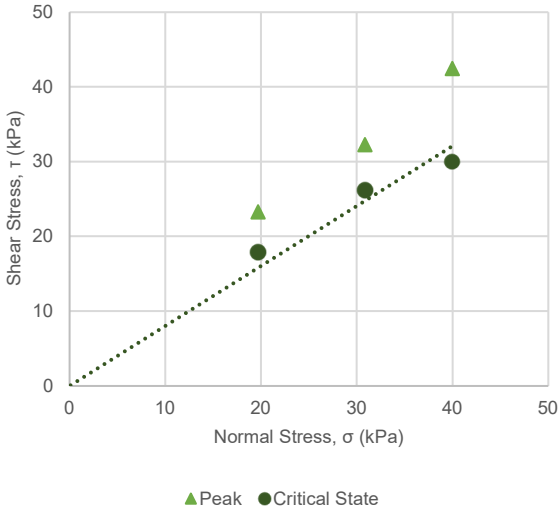

Figure 8. Shear stress vs. normal stress plot for the SWR and 28 mils asperity LLDPE geomembrane interface

Table 2. Direct shear results for the SWR and geomembrane interface

Interface Materials	Interface Friction Angle, δ (°)	Dilation Angle, β (°)
SWR, HDPE (16 mils Asp.)	40	6
SWR, HDPE (20 mils Asp.)	38	9
SWR, HDPE (28 mils Asp.)	42	6
SWR, LLDPE (16 mils Asp.)	40	7
SWR, LLDPE (20 mils Asp.)	39	9
SWR, LLDPE (28 mils Asp.)	39	11
SWR, PDG	43	0

5.3 Geomembrane and Planar Drainage Composite Interface

Direct shear test results for the geomembrane and PDG interface showed decreasing interface friction angles and increased adhesion with an increase in asperity height, typically resulting in increased shear strength with increased asperity height. The only exception to this observed trend is the 28 mils asperity LLDPE geomembrane which had the highest interface friction angle and lowest observed adhesion. Interface friction angles ranged from 14° for the 28 mils asperity HDPE geomembrane to 28° for the 28 mils asperity LLDPE geomembrane. Figure 9 presents a typical plot of peak shear stress vs. normal stress for a PDG and geomembrane interface. Results for the geomembrane and PDG interface tests are shown in Table 3.

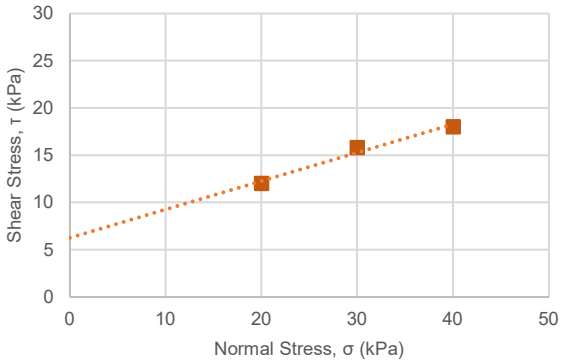

Figure 9. Shear stress vs. normal stress plot for the planar drainage composite and 20 mils asperity HDPE geomembrane interface

Table 3. Direct shear results for the PDG and geomembrane interface

Interface Materials	Interface Friction Angle, δ (°)	Adhesion, a (kPa)
PDG, HDPE (16 mils Asp.)	25	3
PDG, HDPE (20 mils Asp.)	17	6
PDG, HDPE (28 mils Asp.)	14	12
PDG, LLDPE (16 mils Asp.)	23	7
PDG, LLDPE (20 mils Asp.)	16	9
PDG, LLDPE (28 mils Asp.)	28	1

5.4 Displacement to Peak Shear Stress

The displacement of the bottom section of the shear box was recorded at the occurrence of peak shear stress for each test. Displacement at peak shear stress ranged from 6.2 mm to 8.8 mm for the SWR and geomembrane interface. The HDPE geomembranes showed increased displacement at peak shear stress with increasing asperity height, while the LLDPE geomembrane showed the smallest displacement with 20 mils asperity height. Larger displacements were observed with the PDG interfaces with displacements ranging from 12.2 mm to 26.5 mm at peak shear stress. The average displacement at peak shear stress for each set of tests is shown in Table 4.

Table 4. Displacement to peak shear stress during the direct shear test

Interface Materials	Average Displacement at Peak Shear Stress (mm)
SWR, HDPE (16 mils Asp.)	6.5
SWR, HDPE (20 mils Asp.)	7.1
SWR, HDPE (28 mils Asp.)	8.8
SWR, LLDPE (16 mils Asp.)	7.3
SWR, LLDPE (20 mils Asp.)	6.2
SWR, LLDPE (28 mils Asp.)	8.1
SWR, PDG	12.2
PDG, HDPE (16 mils Asp.)	18.1
PDG, HDPE (20 mils Asp.)	15.1
PDG, HDPE (28 mils Asp.)	26.5
PDG, LLDPE (16 mils Asp.)	24.3
PDG, LLDPE (20 mils Asp.)	23.8
PDG, LLDPE (28 mils Asp.)	24.0

6 DISCUSSION

The measured interface friction angles for all interfaces evaluated in this series of tests were less than the internal friction angle of the SWR. Interface friction angles for the geomembrane and SWR interfaces were measured in a range between 38˚ and 42˚ with no clear relationship to the geomembrane asperity height. Five of the six geomembrane-SWR interface tests showed increasing dilation behavior with larger asperity heights, except for the 28 mils asperity HDPE geomembrane which had the

smallest inferred dilation angle. The geomembrane and PDG interfaces showed decreasing interface friction angles and increased adhesion with increasing geomembrane asperity height, except for the 28 mils asperity LLDPE geomembrane interface.

The unexpected variability in these results at some of the interfaces evaluated highlights the importance of testing the specific materials that will be used in a project. Direct shear testing involving multiple layers of material to mirror site conditions will inherently yield more variability than a direct shear test between two materials. Additionally, more variability could be introduced from manufacturing differences as the geomembranes tested, while all from the same manufacturing company, were sourced from three different manufacturing locations in three different countries.

Evaluation of the results demonstrate that the interface between the geomembrane and PDG will have the lowest friction angle of any interface within the waste rock pile cover system, which is consistent with the results from Bacas et al. (2015) and Cen et al. (2018). Therefore, the geomembrane and PDG interface will govern the slope design so that veneer failure within the cover system is avoided. While this may not be the case for all site conditions and combinations of available materials, geosynthetic-geosynthetic interfaces warrant careful evaluation as a potential point of failure within a cover system.

7 CONCLUSION

A series of direct and interface shear tests were used to evaluate the veneer stability of geosynthetic cover system for mine waste rock. The geomembrane and SWR interface test results showed interface friction angles between 38˚ and 42˚ with no clear relationship to the geomembrane asperity height, and dilation angles between 6˚ and 11˚ typically increasing with asperity height. The geomembrane and PDG interface test results showed that increasing asperity height typically corresponded to decreasing interface friction angles and increased adhesion, resulting in an overall increased shear strength. Some unexpected variability from the observed trends occurred for the geomembrane-SWR and geomembrane-PDG interfaces. These tests identified the geomembrane and PDG interface will govern the selection of a design slope and that geosynthetic-geosynthetic interfaces should be closely examined in any cover system design. The importance of performing testing on project specific materials was also highlighted by observed variability from expected trends.

8 ACKNOWLEDGEMENTS

The authors of this paper would like to thank the Natural Sciences and Engineering Research Council (NSERC) for providing funding for this research and Solmax for providing geomembrane samples.

9 REFERENCES

Abdelaal, F. B., & Solanki, R. (2022). Effect of geotextile ageing and geomembrane surface roughness on the geomembrane-geotextile interfaces for heap leaching applications. *Geotextiles and Geomembranes*, 50(1), 55–68. https://doi.org/10.1016/j.geotexmem.2021.09.001

Adeleke, D., Kalumba, D., Nolutshungu, L., Oriokot, J., & Martinez, A. 2021. The Influence of Asperities and Surface Roughness on Geomembrane/Geotextile Interface Friction Angle. *International Journal of Geosynthetics and Ground Engineering*, 7(2), 1–12. https://doi.org/10.1007/s40891-021-00265-y

ASTM Standard D5321: Standard Test Method for Determining the Shear Strength of Soil-Geosynthetic and Geosynthetic-Geosynthetic Interfaces by Direct Shear. 2021. ASTM International, West Conshohocken, PA, USA.

Bacas, B. M., Cañizal, J., & Konietzky, H. 2015. Frictional behaviour of three critical geosynthetic interfaces. *Geosynthetics International*, *22*(5), 355–365. https://doi.org/10.1680/jgein.15.00017

Cen, W. J., Wang, H., & Sun, Y. J. 2018. Laboratory investigation of shear behavior of high-density polyethylene geomembrane interfaces. *Polymers*, 10(7). https://doi.org/10.3390/polym10070734

Fowmes, G. J., Dixon, N., Fu, L., & Zaharescu, C. A. 2017. Rapid prototyping of geosynthetic interfaces: Investigation of peak strength using direct shear tests. *Geotextiles and Geomembranes*, 45(6), 674–687. https://doi.org/10.1016/j.geotexmem.2017.08.009

MEND, 2012. Cold Regions Cover System Design Technical Guidance Document, Report 1.61.5c. Mine Environment Neutral Drainage (MEND), Canada Center for Mineral and Energy Technology, Canada.

Power, C., Ramasamy, M., MacAskill, D., Shea, J., MacPhee, J., Mayich, D., Baechler, F., & Mkandawire, M. 2017. Five-year performance monitoring of a high-density polyethylene (HDPE) cover system at a reclaimed mine waste rock pile in the Sydney Coalfield (Nova Scotia, Canada). *Environmental Science and Pollution Research*, 24(34), 26744–26762. https://doi.org/10.1007/s11356-017-0288-4

Ramasamy M, Power C, Mkandawire M. Numerical prediction of the long-term evolution of acid mine drainage at a waste rock pile site remediated with an HDPE-lined cover system. *J Contam Hydrol.* 2018 Sep;216:10-26. doi: 10.1016/j.jconhyd.2018.07.007. Epub 2018 Jul 24. PMID: 30093079.

Stark, T. D., Williamson, T. A. & Eid, H. T. 1996. HDPE geomembrane/geotextile interface shear strength. *Journal of Geotechnical Engineering*, 122, No. 3, 197–203.

Triplett, E. J. &Fox, P. J. (2001). Shear strength of HDPE geomembrane/ geosynthetic clay liner interfaces. *Journal of Geotechnical and Geoenvironmental Engineering*, 127, No. 6, 543–552.